Tadeusz Z. Woźniak
Kazimierz Wielki University,
Institute of Technology, Section of Materials Engineering,
Bydgoszcz, Poland

AUSTENITE DOUBLE DECOMPOSITION INTO BAINITE IN HIGH CARBON STEELS

ABSTRACT

This paper describes a model of bainitic transformation. The model takes into consideration a range of lower bainite in high carbon steels (the swing back effect near the temperature M_s). The models take into account a simultaneous decomposition of austenite into two transformation products: bainite at the austenite grain boundary and on martensite spines. Analyses concerning the nucleation of sub-plates have been presented. Having two models assumes that the sub-plate growth is of a logarithmic and exponential character. In order to calculate a volume fraction of two components of bainite f_{B1} and f_{B2} , formulas linking an actual volume increase of the components with their current growth have been applied, leading to extended volume. The results of dilatometric studies and quantitative analyses of micro structural components were used in optimizing procedures.

Key words*: bainite, swing back, butterfly, kinetics, simultaneous.*

INTRODUCTION

The bainitic transformation in high carbon steels is characteristic of the accelerated start of the transformation near M_s temperatures. The acceleration of the transition starts in range of temperatures near M_s and is quite clearly evident up to 25% of the transition. Curves corresponding to more than 50% of the transformation show insignificant symptoms of abnormal kinetics, which is related to the formation, of bainite in the further stage of reactions. This phenomenon is undoubtedly caused by the midrib formation which is a twinned martensite. The midrib results in the acceleration of the bainitic transformation as a consequence of the shape deformation of the transformed material area and the local temperature increase. The midrib traces were observed earlier in the martensite in Fe-Ni alloys, where the complementary deformation in the outer parts of the plate does not occur by twinning but by slipping. Transition from twinning to slipping is explained by the local temperature increase at the interface while the inner twinned part of the plate is being formed. The midrib growth is so fast that it runs under adiabatic conditions. Thus, the released heat of transition induces local changes of temperature, which consequently changes the way inner martensitic deformations occur. Heat effects may be accompanied by deformation of the neighboring austenite as a result of the shape deformation of the area which has been transformed. In high carbon steels at adequately high temperatures near M_s, both above factors are favorable for local changes of carbon concentrations in the metastable austenite. The differentiation of carbon concentrations in the untransformed austenite also occurs during bainitic transformation, which has been often confirmed by the results of the research [1-5]. The metastable state may be transformed into a stable one in a few different ways. The way that gives maximum rate of lowering free energy is always privileged. These facts may result in the simultaneous occurence of different transitions induced by diverse thermodynamic conditions in the microareas of the metastable austenite.

The volume increase during transformation in the solid state was described with the use of the classical Johnson – Mehl – Avrami theory, which has been totally verified by Christian [6]. A significant development of Johnson - Mehl – Avrami's theory was the result of the studies made by S. J. Jones and H. K. D. H. Bhadeshia [7]. It enabled T.Z. Wozniak [8] to describe multiple reactions, leading to formation of a microstructure containing two transformation products: bainite at the austenite grain boundary and on martensite spines.

In this study an attempt was made to apply a modified Johnson-Mehl-Avrami theory to multiple bainitic reactions in high carbon steels indicating a swing back effect near temperature M_s. The acceleration of the reaction start near M_s was confirmed by dilatometric tests on 0,85-1,8%C steels and by microstructural tests made by Okamoto and Oka [9,10]. The acceleration was explained by the effect of midrib on the bainitic reaction. A bainite structure consists of fine ferrite plates making aggregates known as sheaves. The plates within each sheaf are parallel and share a common crystallographic orientation. Each plate has a precisely defined habitus plane. Fine plates inside the sheaf are called sub-unites. Their thickness is under one micrometer. Problems concerning the effect of different factors on the width of sub-units and the thickness of plates have been recognized to a small degree so far.

This study is an attempt to create a model of bainitic transformation in the range of accelerated start of the transformation. The model assumes some parameters describing the geometry of the sub-unit. Relative geometric changes of the sub-units as a function of transformation time at different reaction temperatures have been determined. The occurrence of complex reactions made it possible to apply a model of multiple transformations.

ASSUMPTIONS OF THE MODEL OF OVERALL TRANSFORMATION KINETICS FOR TWO SIMULTANEOUS REACTIONS OF DECOMPOSITION

If the geometry of the growing phase is similar to that assumed in the advance model, the measurement of transformation rate changes may occur very helpful while analyzing the transformation mechanism. Relatively, the simplest situation is found when the geometry of the growing phase stays unchanged during the transition, and the migration rate of the transformation front is constant. The transformation rate can be defined in different ways according to the needs. In a simple geometric system, the phase transition runs as a result of movement of the interface S_V with a constant rate $\overline{R}$. The assumption that $\overline{R}$=const is equivalent to the statement that dy/dt=const within the range of changes in the reaction fraction 0<y<1.

For multiple phase transitions, the interface migration rate $\overline{R}$ also changes in time. Thus, the transition rate equation in its most general form is as follows:

$$\frac{dy}{dt} = S_V(t)\overline{R}(t) \tag{1}$$

The geometry of the growing phase is usually very complex and varies in the process of transformation. Due to continuous nucleation, new particles keep on appearing, which makes the sizes considerably differ from one another. At the final stage of the transition, the particles partly prevent each other from their further growth. With the more complex geometry of the system, the total interface S_V changes with time. The function $S_V(t)$ is defined mostly by the geometry of phases growing during the transformation and therefore may change even when the same phase transition runs in different conditions. Besides, the changes of specific surface of the transformation front are sometimes dependent on both the nucleation mechanism and growth of the new phase particles. Thus, an event with a constant rate of interface dislocation $\overline{R}$, dy/dt is a complex function of time. During phase transformations S_V should initially increase rapidly to achieve maximum and then decrease as a result of particle collisions. These effects are particularly noticeable in the range of swing back [11]. The complex function of time dy/dt is also a result of the mutual overlapping of different mechanisms of both nucleation and the bainite sub-plate growths. Consequently, the experimentally determined activation energy of transformation may be of a univocal physical character only in a few cases. When the transformation occurs at considerable overcooling, which is conducive to the reduction of nucleation sites, the determined activation energy becomes the activation energy of the interface migration. While the processes of nucleation and growth run simultaneously for a longer time, the activation energy is merely a defined mean for both the processes [12,13]. It has been stated that at the transformation temperatures within the range of swing back, the kinetic curves are of different shapes. This is a result of the mutual overlapping of two different kinetic curves. According to Z. Kędzierski [14], it is impossible to apply data determining a correct activation energy if the shapes of the curves change. This especially results from the fact that the change of temperature induces the change of the transformation mechanism, which changes the activation energy.

Considering the above conditions, further analyses of bainitic transformation in the range of swing back take into account separately the aspects of nucleation and growth. These parameters have been defined individually for two mutually overlapping phase transitions.

A bainitic transformation usually begins on austenite grain interfaces and is the result of the nucleation and growth of individual plates of bainite. A dislocation taking place during the growth causes the change in the shape. This shape deformation is an invariant-plane strain (IPS) with a large shear component. The growth of plates is inhibited by the concentration of dislocations formed by plastic accommodation. The plates grow to a limiting size. The further transformation makes new parallel plates grow in aggregates called sheaves [15-17], which is presented in Fig. 1. In the models so far, the assumption has been made that the kinetics of the growth and the mechanism of the sub-unit nucleation are the same in all sheaves. The research made by G. Spanos, H.S. Fang, H.I. Aaronson [18] suggests a differentiated mechanism of the sub-unit nucleation. A single plate, which is carbide free to a large extent, forms a spine at the beginning of the whole sheaf of bainite. Then new sub-units are formed by sympathetic nucleation and predominantly on one side, being located app. 55 to 60 degrees in relation to the longitudinal axis.

A complex mechanism of the bainitic transformation in the range of swing back also forms a base to assume that the mechanism of nucleation and growth of two different sheaves is differentiated in the model. At temperatures of transformation below M_{si}, the sheaves being formed initially are of the butterfly morphology. In the model they were marked schematically as B1 and B2. We assume that the two structural components B1 and B2 precipitate simultaneously from the adjacent phase made by austenite. The nucleation rates of the sheaves have been marked, respectively: I_{B1} and I_{B2}. However, the nucleation of the first sub-unit induces both the secondary processes of nucleation and the processes of autocatalysis, which results in the formation of a sheaf. Actually, the number of nuclei formed per volume unit is not constant. It has been assumed that the nucleation rate increases linearly together with an increase in the transition fraction, differently for the sheaves marked B1 and B2. This fact is to be described by coefficients A1 and A2. Thus, the nucleation rate of the sub-units in volume is defined, respectively, as: $I_{B1} \cdot (A1 \cdot f)$, and $I_{B2} \cdot (A2 \cdot f)$. A complete process of nucleation for sheaves B1 is described as:

$$I_1 = I_{B1}(1 + A1 \cdot f) \tag{2}$$

and for sheaf B2 as:

$$I_2 = I_{B2}(1 + A2 \cdot f) \tag{3}$$

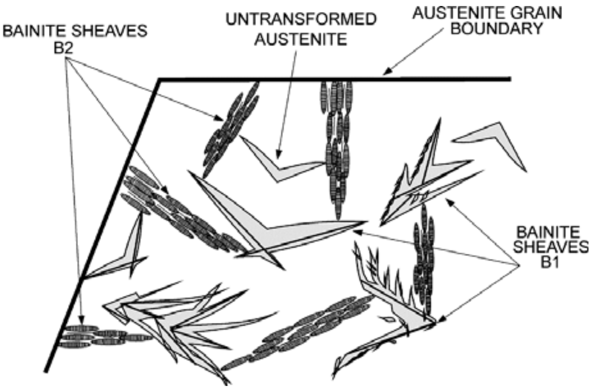

Fig.1. Model of forming two different types of sheaves of bainite B1 and B2 with ellipsoidal sub-units in sheaves at the austenite grain boundary and on martensite spines

It is generally known that sub-units grow with no diffusion and some amount of carbon passes into the residue austenite [19,20]. Since the time necessary for the sub-unit growth is relatively short compared with that required for the nucleation of the next sub-units [20,21], it has been assumed that the time of the sub-plate formation is infinitely low. Thus, the growth rate of the individual sub-units is much higher than the elongation rate of all sheaves [20-23]. The overall kinetics of the transformation include a simultaneous growth and impingements of many sub-plates and then sheaves.

KINETICS OF TRANSFORMATION WITH LOGARITHMIC-EXPONENTIAL GROWTH OF SUB-UNITS

Let us mark constant grow rates for plate B1 in direction “a” and “c” as G_{B11}, G'_{B12}, and a nucleation rate as I_{B1}. Analogically for plate B2, we assume markings G_{B21}, G'_{B22} and I_{B2}. In the model, we also assume that the thicknesses of successive sub-plates in sheaves B1 have the exponential function of time logarithm $a=(G_{B11})^{\ln t}$, and their lengths have the exponential function $c=(G'_{B12})t^{n1}$, analogically, for sheaf B2 $a=(G_{B21})^{\ln t}$ and $c=(G'_{B22})t^{n2}$. Having considered the above assumptions, a sub-plate volume “w” of bainite B1 and B2 in time t=τ is given by the equations (4) and (5):

$$w_{B1\tau} = (\frac{4}{3}\pi)[G_{B11}{}^{\ln(t-\tau)}]^2[G_{B12}{}'(t-\tau)]^{n_1} \tag{4}$$

analogically:

$$w_{B2\tau} = (\frac{4}{3}\pi)[G_{B21}{}^{\ln(t-\tau)}]^2[G_{B22}{}'(t-\tau)]^{n_2} \tag{5}$$

The volume increase resulting from the nucleation of sub-plates B1 and B2 in a time interval t=τ to t=τ+dτ is described by the equation (6) and (7):

$$dV_{B1}^{e} = w_{B1\tau}I_{B1}Vd\tau \tag{6}$$

$$dV_{B2}^{e} = w_{B2\tau}I_{B2}Vd\tau \tag{7}$$

where V is the total sample volume. After substituting (4) into (6), integrating and taking limits into account, we get the equation (8):

$$V_{B1}^{e} = \frac{4\pi V}{3}G_{B12}I_{B1}\frac{1}{\ln C1}\mathrm{Exp}[\ln(C1)\ln(t)] \tag{8}$$

Proceeding analogically as above, we obtain the following formula for B2:

$$V_{B2}^{e} = \frac{4\pi V}{3}G_{B22}I_{B2}\frac{1}{\ln C2}\mathrm{Exp}[\ln(C2)\ln(t)] \tag{9}$$

We assume, that $C1 = G_{B11}{}^2 \cdot \mathrm{Exp}(n_1+1)$ and $C2 = G_{B21}{}^2\mathrm{Exp}(n_2+1)$. In order to integrate the equations, we apply a method of substitution. To calculate the volume fractions of components B1 and B2, formulas were applied connecting the growth of real volumes of the components with their extended volumes [24]. Since B1 is a complex function of B2, analytical integration is not possible unless simplified assumptions, showing relationship between V_{B1} and $V_{B2,}$ are introduced. Following, the assumption that the volume of structural component B2 is a linear function of B1 was incorporated into the calculation and hence $V_{B2} = kV_{B1}$ [24]. Finally, supposing that $V_{B1}/V = f_{B1}$ and similarly $V_{B2}/V = f_{B2}$, by ordering and integrating we obtain:

$$\frac{V_{B1}^{e}}{V} = -\frac{1}{1+k}\ln\left[1-f_{B1}\left(1+k\right)\right] \tag{10}$$

$$\frac{V_{B2}^{e}}{V} = -\frac{k}{1+k}\ln\left[1-f_{B2}\left(\frac{1+k}{k}\right)\right] \tag{11}$$

Considering the equation (8) and (9), substituting it to the equation (10) and (11), we obtain finally:

$$f_{B1} = \frac{1}{1+k}(1-\mathrm{Exp}[\frac{-4\pi(1+k)G_{B12}I_{B1}}{3\ln(G_{B11}{}^2\mathrm{Exp}(n_1+1)}\mathrm{Exp}(\ln(G_{B11}{}^2\mathrm{Exp}(n_1+1))\ln(t))] \tag{12}$$

$$f_{B2} = (\frac{k}{1+k})(1 - \mathrm{Exp}[\frac{-4\pi(1+k)G_{B22}I_{B2}}{3k\ln(G_{B21}{}^{2}\mathrm{Exp}(n_2+1)}\mathrm{Exp}(\ln(G_{B21}{}^{2}\mathrm{Exp}(n_2+1))\ln(t))] \tag{13}$$

For special cases resulting from the calculations, when the thickness of sub-plates is constant $G_{B11} = 1$ and $G_{B21} = 1$, we will obtain simplified forms of equations (12) and (13):

$$f_{B1} = \frac{1}{1+k}(1 - \mathrm{Exp}[-\frac{4}{3}\pi G_{B12}I_{B1}(\frac{1+k}{n_1+1})t^{n_1+1}]) \tag{14}$$

$$f_{B2} = \frac{k}{1+k}(1 - \mathrm{Exp}[-\frac{4}{3}\pi G_{B22}I_{B2}\frac{1+k}{k(n_2+1)}t^{n_2+1}]) \tag{15}$$

The equations (14) and (15) resemble the well-known Avrami equation with the exponential value n+1. The coefficient „k" combines the simultaneous precipitation of two structural components. Considering secondary processes of nucleation in formulas (14) and (15) defined in the equations (2) and (3) by coefficients A1 and A2, and given that $G_{B1} = G_{B12}I_{B1}$ and $G_{B2} = G_{B22}I_{B2}$, we finally obtain:

$$f_{B1} = \frac{1}{1+k}(1 - \exp[-\frac{4}{3}\pi G_{B1}(1 + A_1 f)\frac{1+k}{n_1+1}t^{n_1+1}]) \tag{16}$$

$$f_{B2} = \frac{k}{1+k}(1 - \exp[-\frac{4}{3}\pi G_{B2}(1 + A_2 f)\frac{1+k}{k(n_2+1)}t^{n_2+1}]) \tag{17}$$

KINETICS OF TRANSFORMATION WITH DOUBLE EXPONENTIAL GROWTH OF SUB-UNITS

In the model presented here, it is assumed that the lengths *c* of the successive sub-units and their thicknesses *a* are exponential functions of time (t-τ). The displacement of an interface requires the atoms of the parent to transfer into and adopt the crystal structure of the product phase. The ease with which this takes place determines the interface mobility. The movement of the interface is said to be a diffusion-controlled process. Most of the free energy is dissipated in carbon diffusion. Here, the length $w_{B\tau}$ of plate is a function of $t^{0.5}$ [25]. The interface-controlled growth occurs when the larger proportion of the free energy is consumed in the transfer of atoms across the interface. For this case, the length $w_{B\tau}$ of a plate is a function of $t^{1.0}$. Both processes, diffusion and mobility, dissipate the available free energy and so the motion is under a mixed control. So it is assumed that the lengths $w_{B\tau}$ of successive sub-units and their thicknesses in the time interval dt_u are exponential functions of time (t-τ), according to [26].

The constant growth rates for sub-plate B1 in directions *a* and *c* of the sub-plate are G_{B11}, G_{B12}, respectively, and the nucleation rate is I_{B1}. For sub-plate B2, the corresponding terms are G_{B21}, G_{B22} and I_{B2}. According to [26], it is assumed that the lengths of successive sub-plates and their thicknesses are the exponential functions of time (t-τ). In sheaves B1 c=$(G_{B12})t^{n1}$ and a =$(G_{B11})t^{n3}$, respectively, analogically for B2 c=$(G_{B22})t^{n2}$ and a =$(G_{B21})t^{n4}$, where n_1, n_2, n_3, n_4 are exponents. Considering the above assumptions, a sub-plate volume w of the bainite B1 and B2 in time $t>\tau$ is given by:

$$w_{B1\tau} = (4\pi/3)[G_{B11}(t-\tau)^{n_3}]^2 G_{B12}(t-\tau)^{n_1} \tag{18}$$

$$w_{B2\tau} = (4\pi/3)[G_{B21}(t-\tau)^{n_4}]^2 G_{B22}(t-\tau)^{n_2} \tag{19}$$

where τ is the incubation time. By substituting equation (18) and (19) into equation (6) and (7), integration and taking limits into account, it follows that:

$$V_{B1}^{e} = \frac{4\pi V G_{B11}^{2} G_{B12}}{3(2n_3+n_1+1)} t^{2n_3+n_1+1} \tag{20}$$

and

$$V_{B2}^{e} = \frac{4\pi V G_{B21}^{2} G_{B22}}{3(2n_4+n_2+1)} t^{2n_4+n_2+1} \tag{21}$$

On substituting equation (20) into equation (10) and considering the secondary processes of nucleation defined by coefficients A_1 and A_2 leading to shape plates in the form of a sheaf, we get:

$$f_{B1} = \frac{1}{1+k}\left(1-\exp\left[\frac{-4\pi(1+k)G_{B11}^{2}G_{B12}}{3(2n_3+n_1+1)} I_{B1}(1+A_1 f)t^{(2n_3+n_1+1)}\right]\right) \tag{22}$$

Proceeding analogically as above, we obtain the following formula for B2:

$$f_{B2} = \frac{k}{1+k}\left(1-\exp\left[\frac{-4\pi(1+k)G_{B21}^{2}G_{B22}}{3k(2n_4+n_2+1)} I_{B2}(1+A_2 f)t^{(2n_4+n_2+1)}\right]\right) \tag{23}$$

When n_3 and n_4 equal zero as results from computations, much simpler equations are obtained. These results indicate that the thickness of sub-plates is constant. Given that $G_{B1} = G_{B11}^{2}G_{B12}I_{B1}$ and $G_{B2} = G_{B21}^{2}G_{B22}I_{B2}$, we finally obtain the same forms of equations as in (16) and (17).

EXPERIMENTAL PROCEDURE

Hypereutectoid 1.1% carbon steel was the model material used in the experiment. The steel was delivered in the form of rolled bars of size 30 x 50 mm in a softened state made of the same industrial cast. The chemical content was analyzed by using the appliance „Spectrolab".

In order to make kinetic curves and TTT diagrams showing the range of the accelerated start of the transformation while austempering in the range of M_s, dilatometric and supplementary quantitative analyses were made determining a volume fraction of bainite and the residual austenite. Microstructural observations were carried out on dilatometric samples and on samples of 3 mm diameter after austempering in salt or oil. Microsection etching was done with the use of Vilell's reagent [27]. Dilatometric tests were carried out by using a Adamel Lhomargy 04 dylatometer, applying enlargements: 1000x and 2000x. Depending on the rate of bainitic reaction, the applied time bases ranged from 2 s/cm to 20 min/cm. Samples of size 12x3x0,5 mm were used for the tests. The samples were austenitized in a dilatometer tungstic furnace at temperature 950^{o}C for 30 minutes with a data recording precision 5^{o}C, which resulted in a complete carbide dissolution in the austenite. The samples were heated with a rate of 10 K/s. Austempering was conducted at temperatures from 130^{o}C up to 250^{o}C. The time of withstanding at the isothermal transformation temperature was dependent on the temperature of tests. At temperatures near M_s the time was about 14 hours. Sample cooling from the austenitizing temperature to temperatures of austempering was realized by blowing helium, the flow of which was adjusted by a programmer - controlled electromagnetic valve. Temperature was measured by using thermel welded with a sample.

In order to determine a bainite volume fraction, a microcomputer microstructure analyzer type VFG-512 was used, in which a program with a method of random secants was applied. While analyzing the microstructures on the images the measured areas were separated, to allow 1000 secants in total to be obtained. The values of quantitative volumes of the bainitic phase and the austenite volumes in the dilatometric samples made it possible to properly assess the volume fraction of the product as a function of time while austempering. Diagrams showing the measurements of the dilatometric effects were also used for the assessment.

In order to find equations and kinetic curves for the two reactions running simultaneously, an approximation problem was solved. It resulted from a physical model associating the kinetics of transformation with the bainitic sub-plate growth. The least square method was taken as a test for convergence. To make the estimations mentioned above, a computer program was written, the advantages of which are clarity and the possibility of data processing within the least error S. The program was written in the C++ language and processed into an object oriented form in the Delphi program. An algorithm and the graphic interface of the program enable the user to get sequent results with smaller and smaller errors, without going into theoretical assumptions of the model. The program service is modeled on typical Windows applications and thus it is intuitive and user friendly. The input data are loaded into the program in the form of text files. It is possible to realize calculations simultaneously on several files, however, this considerably limits computing rates and is a significant load for the processor.

To separate kinetic curves for both simultaneous reactions of decomposition $f_{B1}=f_1(k\ n1, A1, G_{B1}, t)$ and $f_{B2}=f_2(k, n2, A2, G_{B2}, t)$ taking place during bainitic transformation, complex kinetic curves while austempering determined by a dilatometric method were used. The experimental data were recorded in one dimension table containing times $t_m[i]$ with their volume fractions $f_m[i]$, where $f_m[i]=f_{B1}[i]+f_{B2}[i]$. Since both functions f_{B1} and f_{B2} are expressed by complex algebraic formulas, their solution was time-consuming

The widths of the steps for which the least square error S was obtained were taken into account as a value of the uncertainty range for each parameter. Experimental errors related to the measurements $t_m[i]$ and $f_m[i]$ as well as errors resulting from the assumed computational steps while searching for solutions of both functions f_{B1} and f_{B2} were taken into account in the calculus calculations of errors made by using the method of total differential.

RESULTS OF THE RESEARCH

Basing on the kinetic curves for the tested steel, a part of the TTT diagram for different transformation rates was constructed and presented in Fig. 2 [28, 29].

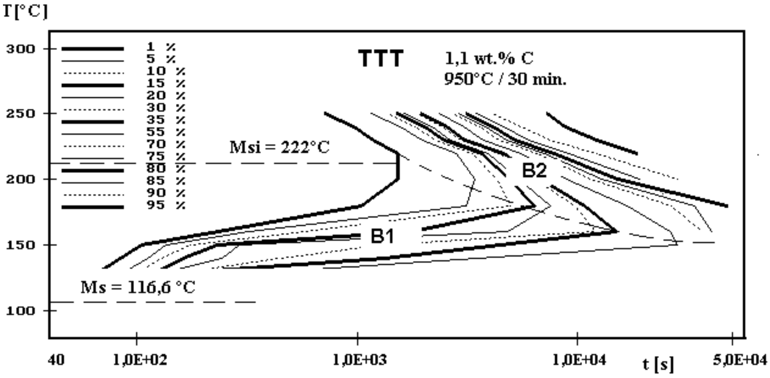

Fig. 2. Fragment of TTT diagram with accelerated starts of transformation at temperatures near M_S

The diagram clearly shows the range of the accelerated start of the transformation near M_s, similarly to the studies of Okamoto and Oka [9,10]. The incubation time of bainitic transformation grows with a decrease in temperature from 250°C to 220°C, whereas with a further decrease in temperature from 200°C to 130°C (above M_s) the incubation time lowers.

The earlier studies [9,10,30] confirmed that in the range of swing back the transformation is of a two-stage character. In the first stage is formed a lower bainite with BDM midrib, and in the other - a classic lower bainite DB. Typical objects of the butterfly morphology were observed best at the transformation temperature of 160°C, Fig. 3.

At this temperature of transformation, the morphology of the objects is the nearest to the model ones presented in literature usually in the context of martensitic transition. Also, considering the transformation conditions, thin threads running along the plates are best observable, which can be seen in Fig. 4 a) and c). The threads are built of previously formed midribs and become thin-plate twinned martensite.

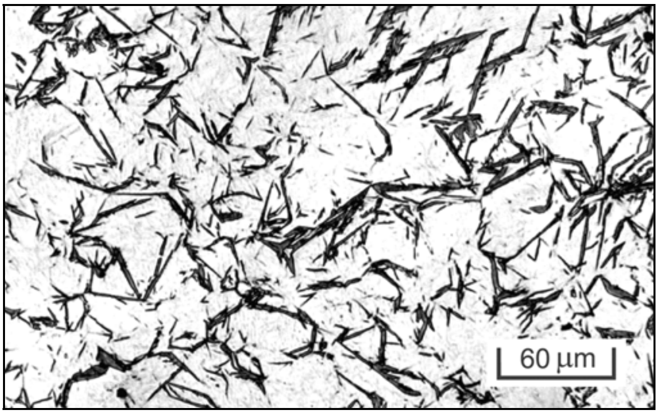

Fig. 3. Optical micrograph after austempering at 160°C after holding time 1800s, volume fraction of bainite: 30%

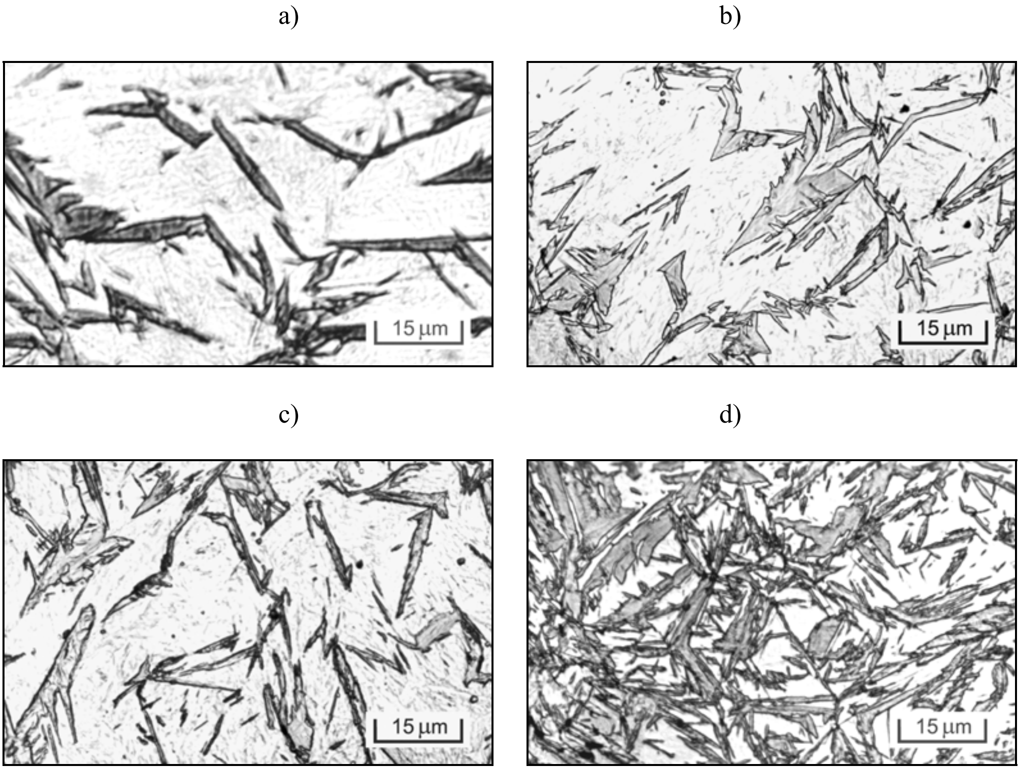

Fig. 4. Substructure of the butterfly bainite after austempering at 160°C, with different holding times a) 300s, b) 864s, c) 1200s, d) 3342s

In Fig. 4 b) and d), the interfacial boundaries of the butterfly bainite plates are irregular. The observations show that it is not only the effect of different cross-sections of these objects but also a more complex morphological structure resulting from the occurrence of the sub-plates. The change in the shape appearing during the bainitic transformation in the vicinity of the sub-plate leads to plastic deformation, which is best proved by the existence of the surface relief.

It has been stated that deformations and tensions influence the butterfly morphology by making the growth of sub-plates active in different planes. The irregular interfacial boundaries may result from the growth occurring in two directions: one longitudinal – by forming sub-plates due to the autokatalysis along the plane $\{252\}\gamma$, and the other – being a result of the preferred growth of some sub-plates along the plane $\{111\}\gamma$.

The two-stage transformation in the tested range of temperatures is observed not only on the kinetic curves but also in the micrographs, Fig. 5.

Fig. 5 presents images of microstructures after a relatively long holding time while austempering. At the lower transformation temperature of 150°C, plates of the butterfly morphology are initially formed and their volume fraction dominates in the structure. After a longer time of the reaction, the second structural component appears, which is typical of lower bainite. However, at transformation temperature of 180°C, the situation is reversed. The butterfly morphology bainite appears in a small number, but a lower bainite of plate morphology is dominant. Only a few microstructural objects of butterfly morphology can be noticed in Fig. 5, being marked as dark places in the background of fine bainite plates, due to their better etching ability.

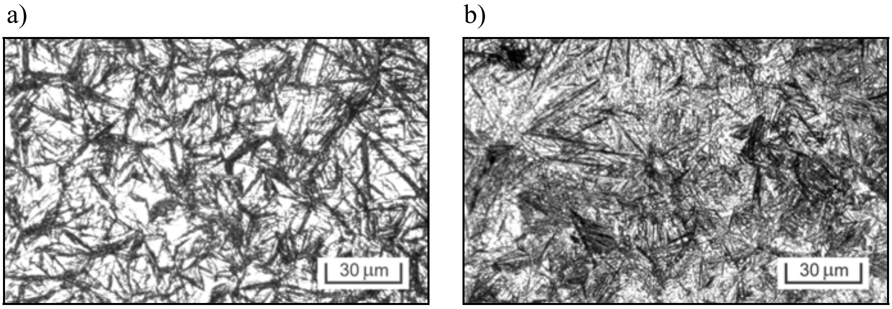

Fig. 5. Optical micrographs after austempering at temperature a) 150°C ,holding time 41030s, volume fraction of bainite 71%, b) 180°C, holding time 51670s, volume fraction of bainite 80.5%

Figures 6 a) and c) show fragments of microstructures with similar volume fractions at transformation temperatures of 130°C and 150°C. At the higher temperature of the transition the volume fraction of microstructural elements of butterfly morphology is lower and numerous fine plates of the lower bainite are observable in the background. Considering the times of transition for the two temperatures, one can notice that the transformation time becomes considerably reduced at the lower temperature along with the same volume fraction, which is the effect of swing back. Fig. 6 b) and d) also present fragments of microstructures with similar volume fractions which were a little smaller than previously, at the transformation temperatures of 140°C and 160°C. Comparing the micrographs, it can be stated that at a temperature of 160^{o}C, a significant fraction of the fine bainite plates is also observable, but at 140^{o}C the butterfly objects are dominant. Taking into consideration the times of transformation, one can notice that the swing back effect disappears at 160°C. It is also observable in the TTT-diagram, in which occurs a repeated swing of the transformation start at temperatures ranging from 160°C to 180°C.

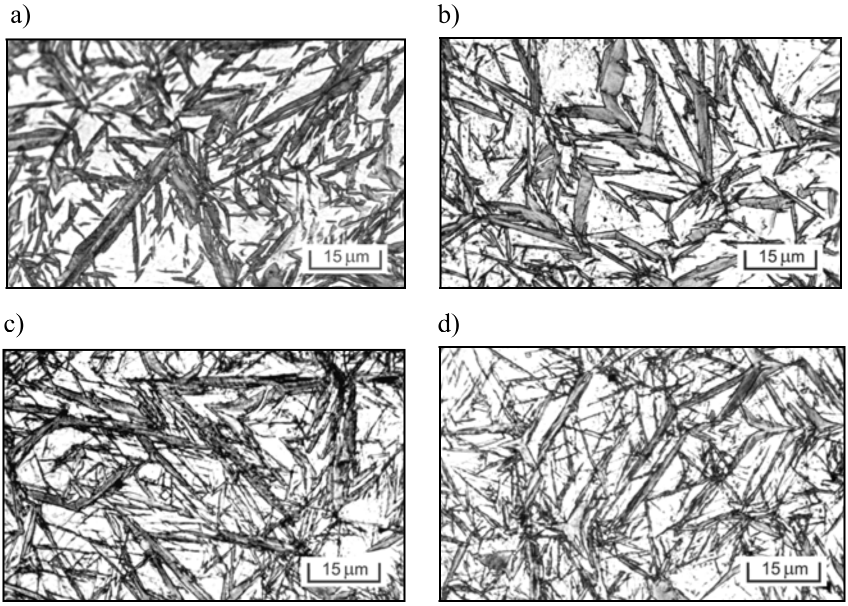

Fig. 6. Comparison of the microstructures with similar volume fractions in the range of swing back in Fig. a), c) and b), d). Austempering at temperature a) 130°C, holding time 8440s, volume fraction 63%, b) 140°C, holding time 34900s, volume fraction 51%, c) 150°C, holding time 40000s, volume fraction 66%, d) 160°C, holding time 15300s, volume fraction 52%

Fig. 7 illustrates two kinetic curves characteristic of austenitic transition while austempering from 130°C to 250°C. After hardening at a temperature of 150°C and after 41030s, the reaction rate was 0,65, whereas after quenching at 250°C and after 8390s, the transformation rate was 0,96. A kinetic curve at 250°C has a typical characteristic sigmoid shape. The accelerated start of transformation and a complex character of the transition resulting from simultaneous occurrence of different reactions can be observable on the kinetic curves at 130°C to 160°C.

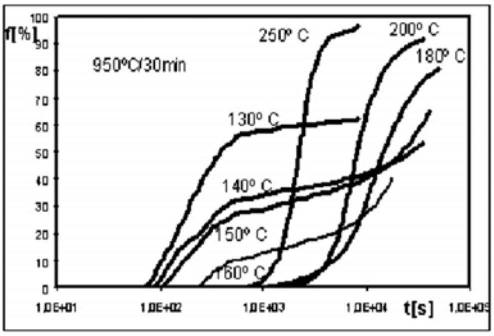

Fig. 7. Kinetic curves at isothermal transformation temperatures from 130°C to 250°C

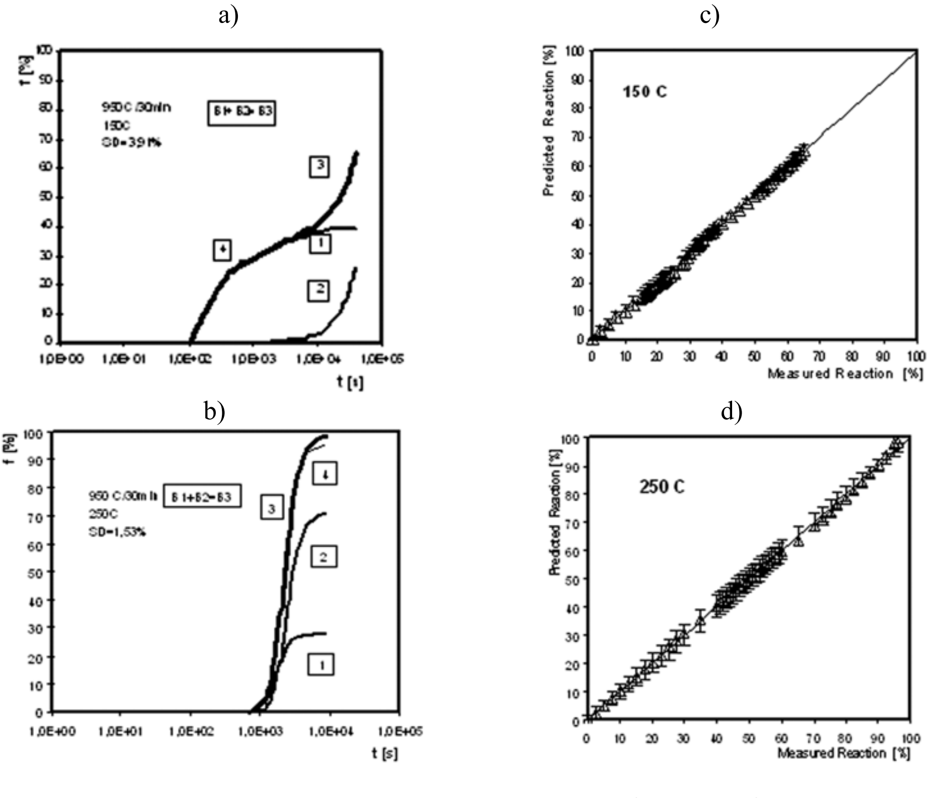

Fig. 8. Distribution of kinetic curves no. 4 for transformation temperatures of a) 150° C and b) 250°C into two curves according to the model of two simultaneous reactions marked as no.1 and no.2. The figures c) and d) show a standard deviation SD indicating a precision of description for the experimental curve no. 4. The model curve no. 3 being a sum of curves no. 1 and no. 2. Maximum errors determined by the method of total differentiate are marked in the diagrams on the right hand side

Basing on the calculations, equations have been obtained which help to plot kinetic curves separately for both reactions of decomposition f_{B1} and f_{B2}. These curves were determined for different temperatures of austenite decomposition and were marked, respectively, no. 1 and no. 2 in Figure 8. The curves marked no. 4 present experimental data f_m, and those marked no. 3 - predicted data f_p being a sum of the function f_{B1} and f_{B2} for both reactions of decomposition. In figures neighboring on the kinetic curves, the results of error calculus were shown. The figures present experimental data and the data predicted on the basis of calculations using the function f_p. The plots include maximum errors calculated by applying the method of total differential.

DISCUSSION OF THE RESULTS

It is generally assumed that due to the changes in temperature, the overcooled austenite decomposition may occur by means of different processes. One of them engaging diffusion leads to the formation of stable mixture of ferrite and cementite. The other one, diffusion free, gives a metastable component called martensite. While lowering the temperature, the reaction rate of the first one rapidly decreases, whereas the other one, diffusion free, is much less dependent on temperature. Consequently, at low temperatures, the rate of diffusion processes is practically near zero and the diffusion free transformation occurs.

Phase transformations at temperatures in the range of swing back are not isokinetic ones due to the changeable mechanism of the transition. To illustrate, for isokinetic transformations, the character of the function f(y) does not change with changes in the transformation temperature. The diagrams presented in Fig. 9 show that extremum (dy/dt) do not appear at the same values $y=y_0$, which confirms that the transformations are not isokinetic.

The assumptions to the model presented above suggest that a general function of the reaction rate is a complex function of time dependent on the effect of changes both in the geometry of phases formed during the transformation and in the migration rate of the transformation front. These effects are visible in the diagrams presenting changes of rates at two ranges of transformation temperatures, Fig. 9 a, b. For bainitic transformation, a character of changes in the reaction rates, clearly seen in the diagrams, is also caused by simultaneous mutual overlapping of the different phase transitions. This is the result of carbon concentration changes and different termodynamic conditions in local micro-areas of metastable austenite.

There is very little evidence indirectly confirming heterogeneous carbon distribution in the untransformed austenite, after completing the isothermal bainitic transformation. The research made by Bhadeshia [4] analyzing carbon contents in austenite with a X-ray microprobe combined with a high-resolution spectrometer proved the existence of heterogeneous carbon distribution in austenite. Matas and Hehmann [5] also observed the occurrence of two different parameters of residual austenite lattice, corresponding with different carbon concentrations in austenite within the area of one sample. However, in many cases austenite undergoes martensitic transformation while being aftercooled to the ambient temperature. Later measurements of carbon concentrations in residual austenite with the use of X-ray methods may lead to the overestimation of x_γ. Thus, the analysis of the transformation kinetics is one of the methods for estimating heterogeneity at isothermal transformation temperature in metastable austenite. As has been shown, these phenomena particularly appear in high carbon steels in the range of swing back with a midrib being an initiator of the bainitic transformation. The midrib induces not only the reduction of the incubation period but it also accelerates a general rate of the transformation.

Depending on the accepted assumptions about the geometry of phases and the conditions of the nucleation and growth, it should be stated that the specific form of the Johnson and Mehl equation significantly changes [11]. However, in each case the curve presenting a change of the reaction rate in time shows the so called “sigmoidal” shape. When the transformation mechanism does not change, the kinetic curves are identical, being translated at different temperatures of transformation. For bainitic transformation in the range of swing back, these curves not only change their slopes during translation but also show a two-stage character, which is clearly seen in Fig. 7. The figure shows the experimental kinetic curves with different transformation temperatures. The shape of the curve at the lower transformation temperature clearly indicates a complex process of austenite decomposition. It leads to form bainite of a different morphology. Such a shape of the kinetic curves was confirmed by other research [9,10,30]. Kinetic curves at higher transformation temperatures (160°C – 250°C) have a typical sigmoid shape, which could suggest a homogeneous type of the reaction in the whole range. However, the presented results of the calculations indicate that, despite the actual model shape, these curves are a complex of two separate ones, Fig 5. In the lower range near M_s a clear acceleration occurs related to the effect of midrib.

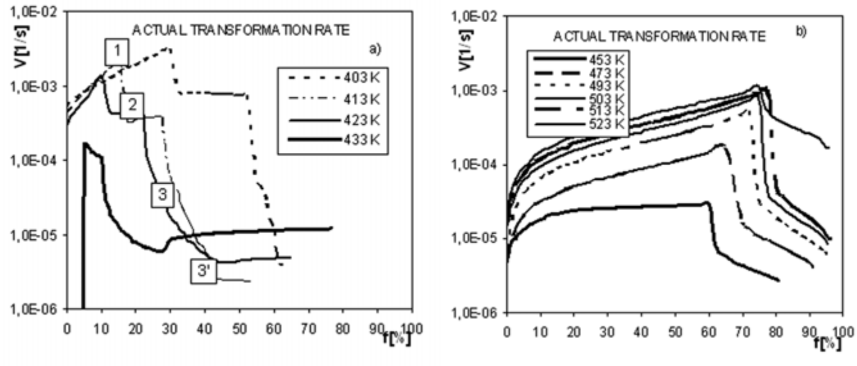

a) b)

Fig. 9. Actual transformation rates during austempering as a function of volume fraction at temperatures: a) 403K-433K; b) 453K-523K

Figure 3 presents a TTT diagram, in which the range of the accelerated start of transformation can be clearly seen. Although such a shape of the plots was many times confirmed in literature, the reason of this phenomenon and its mechanism of the transformation have not been fully explained so far. Undoubtedly, significant results of the research concerning the occurrence of swing back in high-carbon steels were achieved by Okamoto and Oka [9,10]. They stated that in the range of swing back at the start, a midrib being thin-plate martensite is formed, preceding the formation of lower bainite.

The analysis of the reaction rate changes presented in Fig. 9 has been made by using the Johnson-Mehl equation. It is known that several simplifying assumptions have been introduced into the equations:

a) The nucleation and growth of new phase particles run simultaneously during the whole time of the transformation;
b) The distribution of the nuclei in the volume of the input phase is totally random;
c) The nucleation rate is constant;
d) The particles of the new phase nucleate and grow sphere-shaped and their linear rate of growth $\overline{R}$ does not change in time.

At the initial stage, a significant effect of midrib on bainitic transformation can be observed. The lower the temperature of the transformation the stronger the effect. The definition of the mathematical functions describing the character of changes of a specific surface of the transformation boundary and its migration rate in time in the range of swing back goes beyond the present scientific possibilities.

Considering the above, T.Z. Wożniak [13] suggested a method determining the activation energy separately for individual fragments of the transformation by their approximation to the maximum reaction rate. The fragments relate to the transitions for the subsequent stages and different temperatures. The final attribution of these fragments to the particular transitions has been solved by their grouping, applying the least square method.

In equations 3.13 and 3.14 defining the kinetics of growth of sub-units during austenite decomposition, coefficients G_{B11} and G_{B21} appear. The coefficients are related to the „a" parameter defining the thickness of the sub-units. In the first model, there was an important result of computations: $G_{B11}=G_{B21}=1$. It gave a particular value to the plate thickness. The introduction of the obtained results of computations into expressions: 2.13 and 2.14 simplified considerably the final form of the mathematic formulas. In order to avoid controversies, the same forms of the growth functions have been applied to parameters describing the plate thickness in sub-unit. In the first model for element B2, $a=G_{21}{}^{\ln(t-\tau)}$, and for B1, $a=G_{11}{}^{\ln(t-\tau)}$. In the second model for element B2, $a=G_{21}(t-\tau)^{n4}$, and for B1, $a=G_{11}(t-\tau)^{n3}$. We obtain the same results as previously with values $n_4=0$ and $n_3=0$, similarly to the previous case with $G_{B11}= G_{B21}=1$. The particular thickness is only consistent with experimental data from computation and is in accordance with the results obtained by Singh and Bhadeshia. Summing up: in first model $G_{B11}= G_{B21}=1$ and in second model $n_4=0$ and $n_3=0$, are the results of computations that give a particular value to the plate thickness.

In the first model, variations in lengths c of the subsequent sub-plates for each transformation product f_{B1} and f_{B2} are described by respective coefficients: n1 and n2. In the second model, the same functions $G(t-\tau)^n$ have been assumed for parameter c. Owing to the reference of the parameter c to the time $(t-\tau)$, the parameters n_1 and similar n_2 inform about the lengths of sub-units formed individually.

The growth aspect of the problem has been omitted in many treatments concerning overall kinetics controlled by the nucleation rate. In the case of the diffusion-controlled process of length, there is function $t^{0.5}$, and for the interface controlled process – function $t^{1.0}$. The sub-unit growth in bainite takes place much faster than when controlled by carbon diffusion. The circumstances presented above induced the author to apply the growth functions describing the parameters a and c in the form of $G(t-\tau)^n$. In literature, a function $G(t-\tau)^{1.0}$ is often applied to define the sub-unit growth. If that function were universal, in this case the coefficients n_1 and n_2 should have values equal 1.0. In computations in which a prior dictated value of 1.0 for n_1 and n_2 was applied, we obtained high standard deviations. Therefore, considering this case, it is not possible to impose a function describing the growth of sub-unit because the level of precision will not be high enough.

Lately there some data has been published [31] concerning thickening of the bainite sub-plates in relation to the austenite strength, temperature, and chemical driving force necessary for nucleation as independent factors. It was found that the plate thickness is independent of temperature at the stationary level of strength and the driving force ΔG_{max} of austenite. The explicit dependence of the thickness on these variables is not known. Measurement of the lengthening and especially of the thickening kinetics of individual sub-units in sheaves is a difficult problem because of the high resolution required.

The transformation product f_{B1} is definitely applicable to the butterfly morphology and the transformation kinetics of this product is described by curves marked as no. 1 in Fig. 8.

The results confirm the morphological idea of Spanos et al. [18] according to which the nucleation of secondary plates of ferrite takes place across the initiating plate of ferrite called "spine", and the other sub-plates are shorter and shorter.

In the formulas describing the bainite forming kinetics of different morphology f_{B1} and f_{B2}, coefficients of autocatalysis A1 and A2 have been introduced, the aim of which is to respect a change in the nucleation rate along with the increase in the reaction rate.

It is known that the formation of plates leads to elastic and plastic deformations of the matrix. However, it does not result in nucleation of new plates of different orientation, which takes place in case of martensite. Generally, it is supposed that, as far as bainite is concerned, the driving force is enough to form carbon-free nuclei, but in carbon-enriched areas localized around the existed plates, the nuclei cannot be formed. In case of bainite around the plates, a characteristic relief occurs similar to the martensitic one.

The changes in the rate of nucleation due to the autocatalysis are described in the expressions $I_{B1} \cdot (A1 \cdot f)$ and $I_{B2} \cdot (A2 \cdot f)$. To analyze the phenomena, you ought to consider the products of parameters I *A. Parameters G_{B1} and G_{B2} combine the growth rate constants c and the nucleation rate. If we assume that the growth rate constants do not change in time, the parameters G_{B1} and G_{B2} are determined by the nucleation rate, and the products of parameters I *A can indicate an increase as the temperature decreases.

However, the lack of unambiguous interpretation of these effects results from many simplifying assumptions in the mathematic model applied here. Namely, the parameters G_{B1} and G_{B2} combine not only the nucleation rate but also the constants of the growth rates. Moreover, the autocatalysis A1 and A2 has been related to the overall reaction rate $f_{p,}$ but not to the relevant transition volume fractions, separately for each product of transformation f_{B1} and f_{B2}. In the range of the accelerated start of transformation, the autocatalysis related to strain-induced nucleation may play an important role. It is well known that the reaction rate increases extremely fast due to a continuous effect of strain and grows incomparably more significantly than under plastic deformation only.

In the transformation range B1, the parameter b is of order E-4 to E-5, whereas range B2 shows the order E-10 to E-8. When comparing ranges B1 and B2, you can notice that the nucleation rate in the range of swing back for f_{B1} in relation to the range f_{B2} can be higher by six orders of magnitude at low temperatures (130°C) and by three orders of magnitude at high temperatures (250°C). A relative difference in nucleation rates is about three orders of magnitude, which directly determines the effect of swing back.

CONCLUSIONS

1. The first element of the lower bainite plate being formed in the range of the accelerated start of transformation is midrib. The microstructure morphology reveals an arrangement of plates in the shape of a butterfly, and can occur with the so called "tails" or without. The formation of butterfly morphology is preceded by the creation of two crossing one another or weaved midribs being a thin-plate martensite. The butterfly morphology is best identified with low volume fractions of the transformation, **w**ith higher volume fractions this morphology is difficult to identify. A classic lower bainite with characteristic sub-plates is formed at a long time of austempering.
2. The applied model of decomposition takes into consideration geometric parameters of successively formed bainite sub-plates. The implementation of the approximation task

enabled us to solve equations for the two simultaneously running reactions of decomposition in ranges B1 and B2, and to make two separate kinetic curves being the components of one.

3. A precise definition of the parameters is limited by a small number of input variables. The most important assumptions are as follows: a) the volume of structural component B2 is a linear function of B1 in order to apply analytical integration; b) the nucleation rates for each type of sheaf B1 and B2 increase linearly with the growth of the overall volume fraction of bainite in order to simplify the method of computation; c) autocatalytic coefficients related to the changes in nucleation rates; d) the exponential relationship of the volume of the individual sub-plates.
4. Despite the fact that these results provide information about the sub-plate thickness, the equations do not enable us to determine absolute values of parameters a and c for the described sub-unit. This results from the fact that factors G and I are interrelated with one another in variables G_{B1} and G_{B2}, given as a result of the computations.

ACKNOWLEDGEMENTS

The author is grateful to Professor J. Jelenkowski from Technical University of Warsaw, Faculty of Materials Science and Engineering, for helpful and valuable discussion. Appreciation is also expressed to Jeffrey Dobek regarding language corrections. The author also expresses his appreciation to M.Sc.T.Dzikowski for support and helpful work.

REFERENCES

1. Ławrynowicz Z., Barbacki A., *Features of bainite transformation in steels,* Advances in Materials Science 2, 2002, pp. 5-32.
2. Ławrynowicz Z., *Carbon partitioning during bainite transformation in low alloy steels,* Materials Science and Technology, 11, 2002, pp. 1322-1324.
3. Rees G.I., Bhadeshia H.K., *Bainite Transformation Kinetics: Part II. Non-Uniform Distribution of Carbon,* Materials Science and Technology, 8 1992, pp. 994-996.
4. Bhadeshia H.K., Waugh A.R., *Bainite: An Atom-Probe Study of the Incomplete Reaction Phenomenon,* Acta Metall, 30, 1982, pp. 775-784.
5. Matas S.J., Hehemann R.F., *The Structure of Bainite in Hypoeutectoid Steels,* Trans. TMS-AIME, 221, 1961, pp. 179-185.
6. Christian J. W., *Theory of Transformations in Metals and Alloys, Part I,* Pergamon Press, Oxford 1975.
7. Jones S. J., Bhadeshia H.K.D.H., *Kinetics of the Simultaneous Decomposition of Austenite into Several Transformation Products,* Acta Materialia, 45, 1997, pp. 2911-2920.
8. Woźniak T.Z., *Modeling Kinetics of the Austenite Simultaneous Decomposition into Two Bainitic Products in the Range of Swing Back*, Materials Science and Engineering, A, 2005 (in press after recommendation).
9. Oka M., Okamoto H., *Swing Back in Kinetics near* M_s *in Hypereutectoid Steels,* Metallurgical and Materials Transactions, A 19A, 1988, pp. 447-452.
10. Okamoto H., Oka M., *Lower Bainite with Midrib in Hypereutectoid Steels,* Metallurgical and Materials Transactions, A 17, 1986, pp. 1113-1120.
11. Woźniak T.Z., *Kinetic Models of Phase Transformations*, Sci. Bull., No. 241, Mechanics 53, University of Technology, Bydgoszcz 2002, pp. 291-299.

12. Woźniak T. Z, Jeleńkowski J., *Morphology of Lower Bainite in Swing Back*, Proc. Conf. Selection and Utilization of Engineering Materials, Technical University of Gdańsk – Jurata 22-25, September 1997, pp. 207-215.
13. Woźniak T. Z., *Kinetics and Morphology of a Product of Bainite Transformations in the Range of Swing Back,* Archives of Materials Science, 23, 2002, pp. 351-374.
14. Kedzierski Z., *Phase Transformation in Solid State,* AGH, Krakow 2003.
15. Hehemann R. F., *Phase Transformations,* Metals Park, OH, ASM, 1970.
16. Rees G.I., Bhadeshia H.K.D.H., *Bainite transformation kinetics. Part 1 Modified model,* Mater. Sci. and Technol., 8, 1992 pp. 985-993.
17. Rees G.I., Bhadeshia H.K.D.H., *Bainite transformation kinetics. Part 2 Non-uniform distribution of carbon*, Mater. Sci. and Technol., 8, 1992, pp. 994-996.
18. Spanos G., Fang H.S., Aaronson H.I., *A Mechanism for the Formation of Lower Bainite*, Metall. Trans., A 21, 1990, pp. 1381-1390.
19. Christian J.W., Edmonds D.V., *Phase transformations in ferrous alloys,* A.R. Marder and J.I. Goldstein (ed.), TMS-AIME, Warrendale, PA, 1984.
20. Bhadeshia H.K., Christian J.W., *Bainite in Steels*, Metall. Trans., A 21, 1990, pp. 767-797.
21. Bhadeshia H.K., *Growth rate data on bainite in alloy steels,* Mater. Sci. Technol., 5, 1989, pp. 398-402.
22. Bhadeshia H.K., *Phase transformations in ferrous alloys*, A.R. Marder and J.I. Goldstein (ed.), TMS-AIME, Warrendale, PA, 1984.
23. Speich G.R., *Morris Cohen: The growth Rate of Bainite*, Trans. TMS-AIME 218, 1960, pp. 1050-1059.
24. Jones S.J., Bhadeshia H.K D.H., *Kinetics of the Simultaneous Decomposition of Austenite into Several Transformation Products,* Acta Materialia, 45, 1997, pp.2911-2920.
25. Aaron H.B., Fainstein D., Kotler G.R., *Diffusion-Limited Phase Transformations: A Comparison and Critical Evaluation of the Mathematical Approximations*, J. Appl. Phys., 41, 1970, pp. 4404-4410.
26. Reti T., Fried Z., Felbe I., *Computer simulation of steel quenching process using a multi-phase transformation model,* Comp. Mater. Sci., 22, 2001, pp. 261-278.
27. Shui C.K, Rynolds Jr W.T., Shiflet G.J., Aaronson H.I., *A Comparison of Etchants for Microstructures in Fe-C-Mo Alloys*, Metallography, 21, 1988, pp. 91-102.
28. Woźniak T.Z., Jeleńkowski J., *Kinetics of the Austenite Decomposition into Lower Bainite in High Carbon Steels under Austempering Heat Treatments*, Sci. Bull., No. 193, Mech. 38, ATR, Bydgoszcz 1995, pp. 103-110.
29. Woźniak T.Z., *Changes of Bainite Transformation Velocity Formed at Temperatures Near the* M_S *in High Carbon Steel,* 2nd All-Polish Scientific Conference, Technical University of Cracow, 16-18 September, 1999, pp. 171-177.
30. Schaber O., *Some Observations on Isothermal Austenite Transformation Near the Ms Temperature,* Trans. AIME, 203, 1955, pp. 559-560.
31. Singh S. B., Bhadeshia H.K.D.H., *Estimation of Bainite Plate-Thickness in Low-Alloy Steels,* Materials Science and Engineering, A245, 1998, pp. 72-79.